In-situ Bulk Electrophoretic Separation of Single-Walled Carbon Nanotubes Grown by Gas-Phase Catalytic Hydrocarbon Decomposition

Manuscript received: 26/01/2010; Revised: 07/08/2010; Article published: 02/09/2010

In-situ Bulk Electrophoretic Separation of Single-Walled Carbon Nanotubes Grown by Gas-Phase Catalytic Hydrocarbon Decomposition**

D.V. Smovzh,[1,2] V.A. Maltsev,[2] S. Dittmer,[3] V.V. Zaikovsky,[4] E.E.B. Campbell[5] and O.A. Nerushev[2,5,*]

[1]Physics Department, Novosibirsk State University, 630090 Novosibirsk, Russia.

[2]Institute of Thermophysics SB RAS, 630090 Novosibirsk, Russia.

[3]Department of Physics, Göteborg University, 41296 Göteborg, Sweden.

[4]Boreskov Institute of Catalysis, Novosibirsk, 630090 Novosibirsk, Russia.

[5]EaStCHEM, School of Chemistry, Joseph Black Building, University of Edinburgh, West Mains Road, Edinburgh, EH9 3JJ, UK.

[*]Corresponding author; e-mail: Oleg.nerushev@ed.ac.uk

[**]Financial support from the Russian Foundation for Basic Research (project no. 04-03-32143), the Swedish Royal Academy of Sciences (KVA) and the Swedish Strategic Research Foundation (SSF) is gratefully acknowledged.

Keywords:
CNTs; Electrophoresis; Glow discharge; Hollow cathode; Plasma CVD

Abstract

Electrophoresis is used to separate carbon nanotubes from other by-products during CVD growth from iron catalyst particles using C_2H_2 as carbon feedstock. Carbon nanotubes are trapped by electric fields with higher efficiency than other carbon-containing products. The structure and yield of the carbon nanotubes depends critically on the gas parameters and applied electric field used in the novel reaction chamber. A high yield of relatively clean SWNT can be obtained. The results indicate that the nanotubes produced by thermal CVD in the gas phase are negatively charged.

Introduction

Carbon nanotubes (CNTs) are attracting great interest for their remarkable properties and expected utility for nanoelectronics, material science, fuel cells etc. High quality single walled carbon nanotubes (SWNT) and multiwalled carbon nanotubes (MWNT) can be obtained using chemical vapour deposition (CVD) from different carbon sources such as methane, ethylene, other hydrocarbons or carbon monoxide. CVD seems to be the most easily up scalable method for CNT production.

Unfortunately the soot obtained after bulk CVD growth typically contains not only nanotubes, but also a lot of impurities. A challenging problem is to efficiently and cost-effectively purify the CNTs from other forms of unwanted carbon such as graphene flakes, onions and encapsulated catalyst particles. In addition, one would ideally want to separate different forms of CNTs themselves. One of the possible ways is the use of external electric fields for separation of species with different specific surface area, polarisability or surface charge density. Liquid phase electrophoresis was successfully applied for *ex situ* size separation of SWNTs [1] in dc fields and separation of metallic from semiconductor SWNTs [2-4] in ac fields. Earlier, gas phase mobility of carbon cluster ions was widely used for separation of fullerenes from linear and ring-like clusters [5,6]. Recently, electrophoresis in the gas phase was applied for size classification of MWNTs after high-pressure CVD synthesis [7].

In the present article, we demonstrate the efficient bulk production of SWNT in a novel low-pressure CVD reactor combined with an electrophoretic cell. We illustrate for the first time that *in situ* dc electrophoresis can be used to efficiently extract SWNT from other carbon-containing materials produced in the gas phase CVD process. The results indicate that the nanotubes are negatively charged during gas phase growth, providing a powerful tool for manipulation and further purification.

Experimental

Our novel growth reactor exploits a combination of low–pressure gas phase CVD growth with an electrophoretic cell. It consists of a gas feedthrough system, an evacuated bell jar with heated stainless steel

tube and a cylindrical electrode (figure 1). A gas mixture containing the carbon feedstock gas (C_2H_2) and buffer gases (Ar, H_2) is blown through the hot vertical stainless steel tube with a flow rate in the range of 50-100 sccm. Iron catalyst particles are synthesised by thermal decomposition of iron pentacarbonyl directly in the reactor. The pentacarbonyl is delivered to the reaction zone by bubbling C_2H_2 through a vessel containing liquid iron pentacarbonyl at 0^o C. The thermally isolated hot tube is placed inside the vacuum chamber and connected to a vacuum pump through a filter, where carbon soot is collected. The inner diameter of the tube is 20 mm and the length of the hot zone is 180 mm. The gas temperature is measured by a thermocouple suspended on the reactor axis in the gas flow. Pressure is varied by control of the gas flow rate and the pumping speed by inlet and outlet valves. Applying a voltage between the hot tube wall and a retractable coaxial central electrode with a diameter of 1.5 mm can generate an electric field. Most of the experiments were carried out using a bias voltage below the gas discharge ignition point.

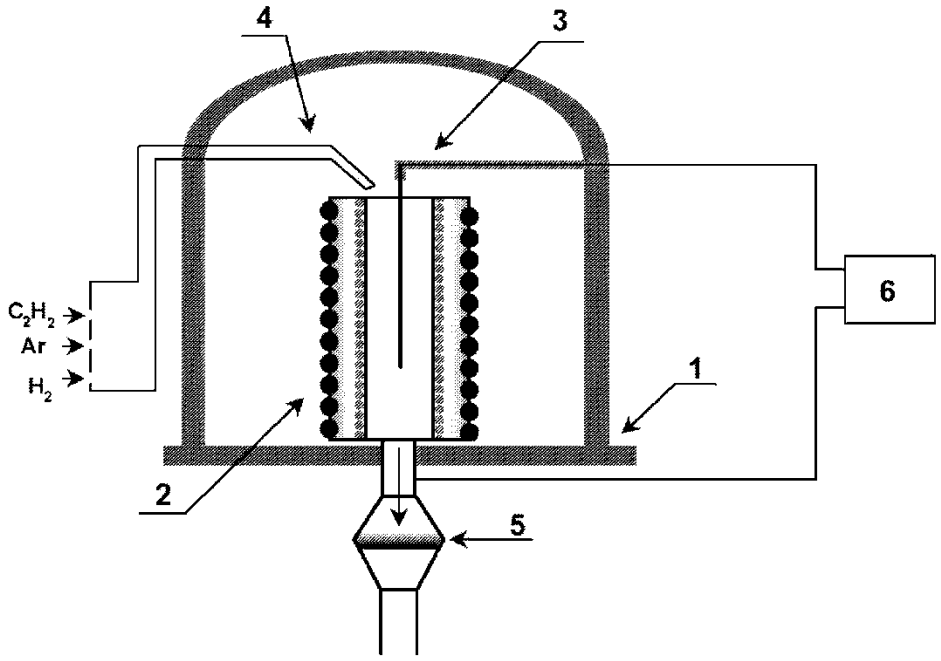

Figure1. Experimental set up.1-Vacuum bell jar, 2- outer heated cylindrical electrode, 3- central electrode, 4- gas feeding system, 5 – filter for floating material collection, 6 – power supply.

The carbon-containing material was collected from the electrodes and the output filter and imaged by scanning and transmission electron microscopy (SEM (JSM 6301F)/TEM (JEM2010)) and investigated by

micro-Raman spectroscopy (inVia Renishaw microscope with 488, 514, 568, 785 nm excitation wavelengths) after dispersion in organic solvents without surfactants.

Results and Discussion

A preliminary set of experiments was performed without the presence of an electric field to determine the range of parameters optimal for CNT production. TEM was used for a qualitative estimation of the dimensions and partial yield of CNTs. Figure2 shows a TEM image of carbon material collected from the filter after an experiment using a $C_2H_2/Ar/H_2$ mixture at 5/80/10 sccm flow rates, respectively, at a pressure of 15 Torr and a temperature of 800^{o} C. Two main fractions of carbon material were found – SWNTs and encapsulated metallic particles. The quantitative analysis of particles responsible for nanotube growth is complicated by the low amount of those particles connected to nanotubes that is visible in each TEM image but we performed the analysis of all metal particles in the field of view. The size distribution of the metallic particles was narrow with a maximum at 2.9 nm diameter and mean square deviation 1.2nm. This size distribution is a consequence of the fast and spatially homogeneous formation of metallic clusters in the gas phase at a small inlet region, combined with a low probability of cluster coalescence in the *hot* zone. SWNTs observed in the TEM have lengths of a few microns. This is surprisingly long considering that the flight time for particles to reach the filter under the experimental conditions should be on the order of 30-100 ms. However, the gas flow dynamics inside the reactor is not well known and the real detention time for growing tubes in the hot zone might be much higher due to possible vortices and small scale turbulence.

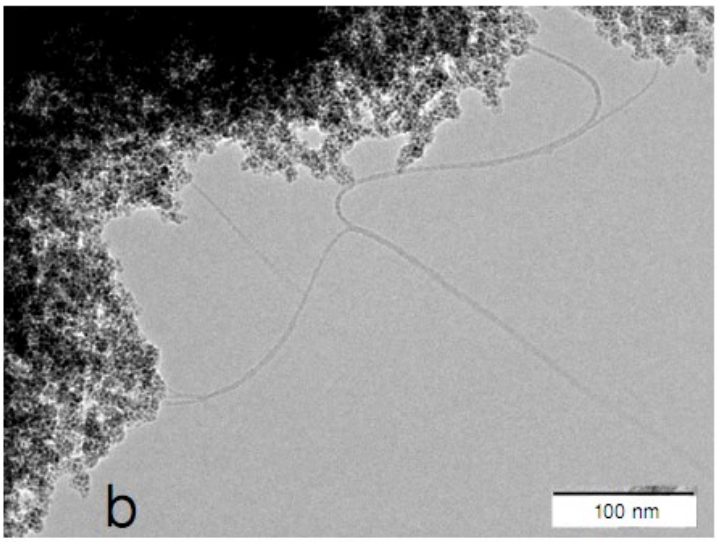

Figure 2. TEM image of low pressure CVD with C_2H_2.

By varying the bias applied to the central electrode we can regulate the electric field in a wide range. Since the specific surface area of CNTs is very high and the drag force from the gas flow depends strongly on this, we can estimate that the extraction of nanotubes from the gas flow will be very inefficient if there is only a small charge on individual CNT. Charge induced on CNTs depends not only on the CNT properties but also on the concentration and temperature of free charge carriers – electrons, positive and negative ions, if any exist in the gaseous environment. The simplest way to increase charge concentration is the ignition of a gas discharge. By placing the central electrode upstream from the heated tube at a distance of 10-15 mm, we obtain a geometry suitable for a hollow cathode gas discharge. The voltage required for the discharge ignition is about 500 V. After ignition, the discharge acts at 200-280 Volts depending on gas pressure, cathode temperature, electric current and load curve of the electric power supply. The discharge current was varied in the range of 0.1 - 50 mA. Power input from the discharge does not exceed 10% of the tube heater power at the highest current and is much less at lower current. Therefore, the influence of the discharge on the gas temperature is negligible. No CNTs were found on the filter after experiments with the hollow cathode gas discharge. TEM investigation of the carbon deposit did not show any changes in the distribution of encapsulated particles compared to the results discussed above, which means that the absence of CNTs is not related to the catalyst transformation. Surprisingly, carbon nanotubes were found on the anode surface placed upstream in the cold zone. These CNTs were not formed at the anode surface but were transported from the hot zone by the electric field. We conclude that the electrophoretic force is large enough to transport the nanotubes even inside the hollow cathode where the electric field is relatively small.

Further investigation was aimed at carbon species separation by using a radial electric field inside the hot tube. The electrode was placed coaxially inside the grounded hot tube. The voltage on the central electrode in the following set of experiments was varied from –150 to +150 V, this is less then the voltage needed to induce electrical breakdown. Soot was collected from both electrodes and filter and investigated with SEM/TEM and micro-Raman for different gas compositions and electric field distributions. At low bias (not higher than 30 V) on the central electrode, a constant increasing of the current up to a level of 0.2 A was registered. We found that the main current channel is a carbon web made from carbon filaments formed at the central electrode. After a few minutes of operation this web became visible with the naked eye. Similar web formation was observed for laser ablation of graphite in the presence of an electric field [8]. The anode with the carbon “ponytail” is shown in the insertion in Fig.3. Time dependence of the current for different polarities of the central electrode is shown in fig.3a. The initial rate of current growth is much less when a negative bias is applied to the central electrode. Also, the amount of material collected from the positive side is much higher for any geometry of electrodes in the case when the web does not fill the whole volume of the reactor and material from the electrodes may be collected separately. If the applied voltage is increased above 50-70 V, the current-time dependence becomes non-monotonic. In this case the current load on the carbon web becomes too high and the filaments explode when they reach opposite electrode. The events of explosion are observed irregularly in time and between them small DC current is also measurable. The value of this current

is irreproducible in different experiments but is constant in one single experiment. That DC component of current corresponds to non-self consistent gas discharge due to the existence of free charge carriers. The temperature is probably too low to attribute the high concentration of charge carriers to thermionic processes, even when considering the energy released during the catalytic decomposition. One possible source could be the formation of ions during decomposition of acetylene on the catalytic particles. This effect became even more pronounced when the bias exceeded the self consistent gas discharge ignition value. Fig. 3b shows the current through the plasma under positive bias (300 V) at the central electrode. The current consists of two parts. Huge vertical peaks correspond to the moments when the circuit is shorted through the carbon web, but, between them, the current returns back to a finite value, which is constant during a few hours of experiment.

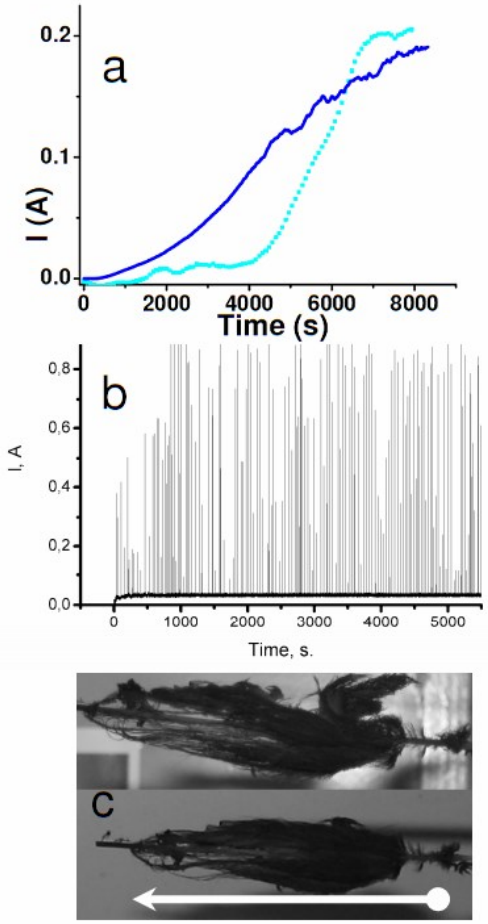

Figure 3. Temporal dependence of current: a) bias 30 volt, solid line - positive polarity of central electrode; dotted line - negative polarity of central electrode; b) Negative polarity, glow discharge, c) illustration of carbon filamentous ponytail collected in central negative electrode after growth with low voltage (30 V), arrow shows the flow direction.

The structure of the soot deposited on the electrodes and filter was investigated by TEM and SEM. Figures 4 a,b,c show SEM images of the material collected from all three parts after an experiment with maximum applied electric field without discharge ignition (voltage +140 V). The absence of any filamentous structures on the filter provides convincing support for the assumption of a strong electrophoretic force acting on the CNTs. The “cathode” material (from the grounded outer cylinder) consists mainly of thick fibres, which may not have grown from the small catalytic particles found in the gas phase, but may have been grown directly on the stainless steel surface or on coagulated nanoparticles deposited on the cylinder wall. The “anode” material (from the central, positively biased electrode) is rich with tiny filamentous structures and small spherical particles. The structure of the material deposited on the “filter” looks closer to amorphous. The SEM images do not provide full information on the carbon deposit composition because of the lack of spatial resolution, making it difficult to observe SWNTs and the problem of distinguishing between bundles of SWNTs and MWNTs. The preliminary experiments without electric field (see above) produced only SWNTs at the filter. A TEM study was performed on the material grown in the presence of a high negative bias on the central electrode without plasma ignition (same material as used for the SEM investigations). The TEM images (figures 4 d, e) show that material from the anode contains mainly single-walled tubes. More importantly, there is a clear difference in the structure of the material collected from the anode and the cathode. The cathode material contains more encapsulated particles and the relative yield of CNTs is much lower than for the anode material.

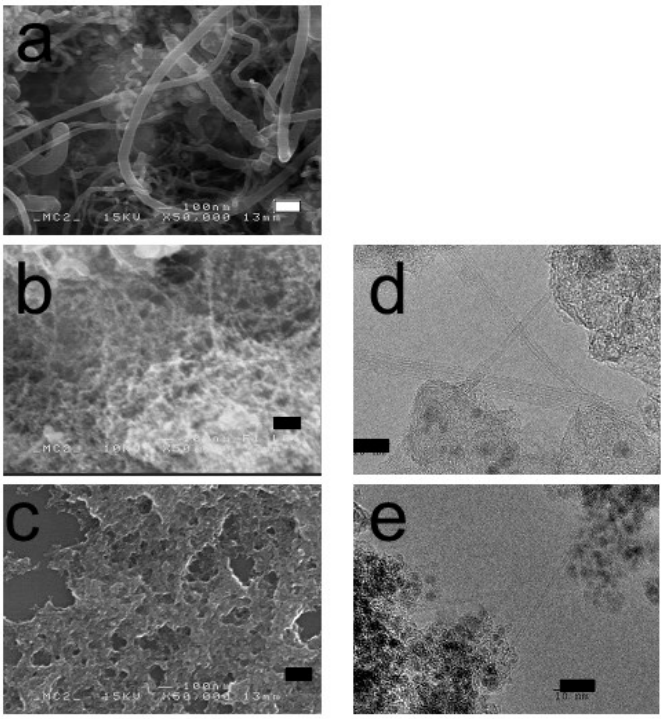

Figure 4. Electron microscopy images of material collected from cathode (a), cylindrical anode (b, d) and filter(c, e). SEM – a, b, c; TEM – d, e. Scale bar: left column 200nm, right column 10 nm

Experiments in which only the magnitude of the bias on the central electrode is changed, do not distinguish between electrophoretic and dielectrophoretic mechanisms of separation. Electrophoresis depends on the magnitude of the electric field and dielectrophoresis depends on the field gradient. In the cylindrical geometry of our set up, the electric potential in the absence of current varies logarithmically from the central electrode to the cylinder walls and the electric field decreases in inverse proportion to the radius. We thus have the strongest electric field and strongest electric field gradient at the surface of the inner electrode.

Experiments with negative potential on the central electrode were carried out for comparison with the experiments above (figure 4), where the central electrode was positively biased, and the corresponding set of SEM/TEM images is shown in figure 5.

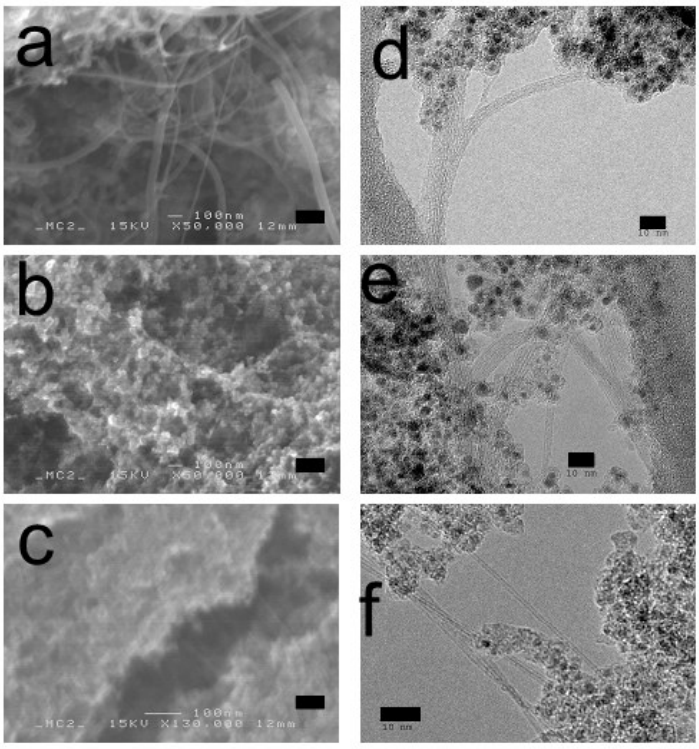

Figure 5. Electron microscopy images of material collected from central anode (a, d), cylindrical cathode (b, e) and filter(c, f). SEM – a, b, c; TEM – d, e, f. Scale bar: left column 200nm, right column 10 nm

The efficiency of electro trapping is almost the same and the material on the filter contains only a very small amount of SWNTs (figure 5 c, f). Surprisingly, the highest enrichment with SWNTs was found again on the positive side although the field value and field gradients were higher at the negative electrode. Thus we infer that the main driving mechanism of the separation is electrophoresis of negatively charged SWNTs. Other important observations can be made. The SWNT found at the reactor wall (the grounded electrode) are

generally covered with amorphous carbon and one can also find MWNT in the material. This is not the case for the material deposited at the central electrode that consists solely of clean SWNT and coated catalyst particles. Moreover, it seems that CNTs during the gas phase synthesis are predominantly negatively charged which may be exploited for *in situ* purification and separation of carbon species. The possible role of carbon anions in the CVD growth of nanotubes on substrates has recently been discussed in the context of enhanced growth of nanotubes from negatively biased electrodes [9].

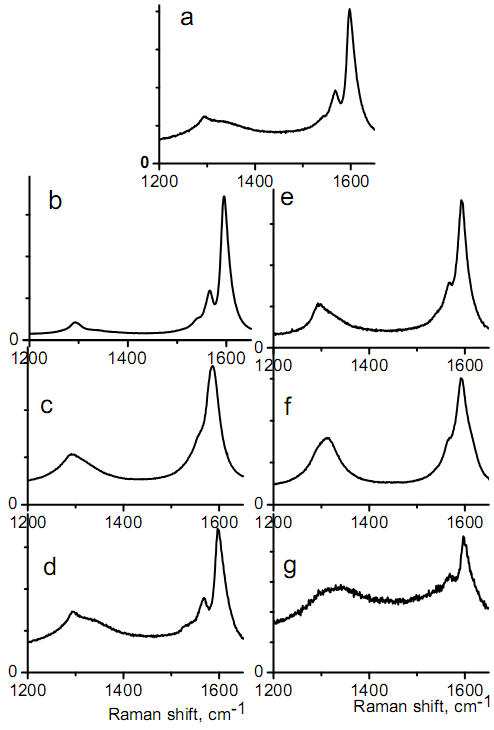

Figure 6. Raman spectra of materials corresponding to SEM and TEM images from figures 4,5.

a- material from filter without applied bias; in columns: b, c, d – material from experiment with hollow cathode, e, f, g – hollow anode; in rows: b, e –material from positive electrode, c, f, - from negative electrode, d, g – material from filter.

Electron microscopy allows us to find qualitative differences between material trapped on electrodes and passed to the filter. Supplementary evaluation of materials may be obtained from optical or infrared spectroscopy. Results of Raman spectroscopy of CNT containing soot are shown in figures 6 and 7. Laser with wavelength 785 nm was used for excitation of Raman scattering in all shown spectra. The comparison of the D (approx. 1340 cm^{-1}) and G lines (approx. 1590 cm^{-1}) in the Raman spectra for non-separated soot and material from the filter and the electrodes for the two oppositely biased electrode configurations is shown in

Fig 6. The relative intensity and relative width of these bands is reproducible for each sample and may be used as a basis for quantitative characterization of the materials. The D line is closely related to the defect –induced D line of graphite and exhibits a weaker resonant enhancement in comparison with other CNT Raman lines [10]. Consequently, the ratio of the D to G peaks corresponds to the number of defects or to the amount of carbon material, which is out of resonance with the excitation laser line. This ratio is decreased for all materials collected from the electrodes in comparison to growth in the absence of an electric field and is increased for material that has passed through the electric field and reached the filter. In the latter case both lines are broadened and have a non-resonant background, which is a consequence of a defective hexagonal structure. Similar results were registered for all excitation lasers used in the Raman measurements.

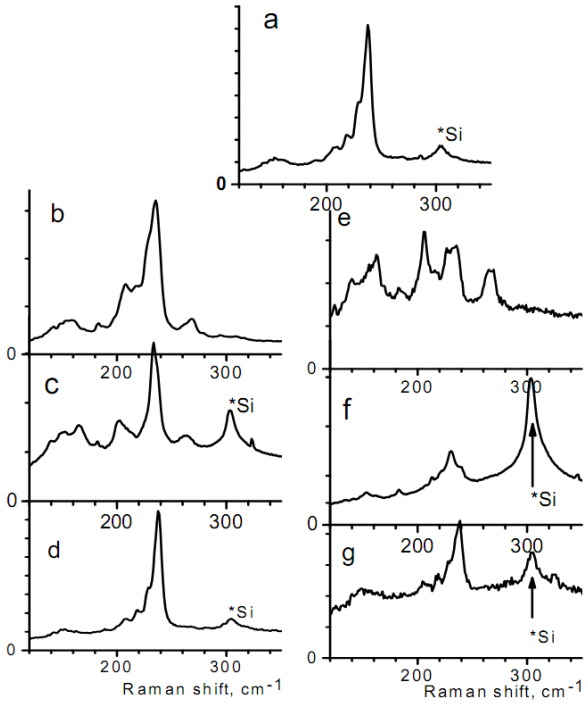

Figure 7. Raman spectra of materials corresponding to SEM and TTEM images from fig.4,5.

Frames designations correspond to figure 6. Low wave numbers range corresponds to radial breathing modes of SWNTs.

The RBM Raman signal in the low wavenumber region of the spectra is representative of the wide distribution of CNT diameters in the samples and is characterized by a significant variation of relative peak intensities across each sample. Reproducibility of those spectra over the whole sample is poorer for the nanotubes that have passed through the electrophoretic separation and have reached the filter. In that case very few lines are visible, and the wavenumbers of these lines are not reproducible across the samples. This is a consequence of

the very low percentage of SWNT in the material, which were not trapped by the electric field. At the same time, the non-resonant background is much higher in comparison to material collected at the electrodes. From the Raman results we cannot detect any significant influence of the electric field on the SWNT diameter distribution function or separation by other properties like chirality or nanotube conductivity. The richest structure of RBM and a higher signal-to-background ratio were registered for material collected from the central anode (Fig 7 b), which is consistent with the electron microscopy study. Appearance of signal from tubes with lower RBM frequency was obtained for material collected from outer electrode (Fig.7c – hollow cathode and Fig.7e – hollow anode). These lower frequencies correspond to bigger diameter of CNTs. Most probably, these larger CNTs were nucleated and grown not in gas phase but in the wall due to trapping and coagulation of catalyst particles. These larger particles may be easier formed on hotter surface, since reactor wall in all cases is slightly overheated in respect to gas flow. Other possible explanation is formation of outer wall on the surface of trapped SWNT but it would contradict to TEM observation.

Conclusions

Partial separation of SWNTs from CVD by-products was achieved directly during production using a novel gas phase CVD method in the presence of an electric field. The main mechanism of carbon species separation is related to electrophoretic motion due to accumulation of electric charge on the tube surface. Negatively charged tubes were found to be dominant. The mechanism of charging is not yet understood, but the effect can be developed for technological applications involving *in situ* purification during bulk nanotube growth. Possibly, the kinetics of the surface catalytic reactions is a key factor to understanding the observed effect and further development of the method.

References

[1] Umek P., Mihailovic D., 2001 *Synth.Met*., **121**, 1211.

[2] Krupke R., Hennrich F., Loehneysen H., Kappes M.M., 2003 *Science,* **301**(5631), 344.

[3] Doorn S. K.; Strano M. S., O'Connell M J., Haroz E. H., Rialon K. L., Hauge R. H., Smalley R. E. 2003 *J. Phys. Chem. B* **107**(25), 6063.

[4] Lee D.S., Kim D.W., Kim H.S., Lee S.W., Jhang S.H., Park Y.W., Campbell E.E.B., 2005 *Appl.Phys. A*, **80**, 5.

[5] Von Helden G., Hsu M.T., Kemper P. R., Bowers M. T. 1991 *J. Chem. Phys*. **95**(5), 3835.

[6] Hunter J. M., Jarrold M.F. 1995 *J. Am. Chem. Soc*. **117** (41), 10317.

[7] Kim S.H., Zachariah M.R. 2005 *Nanotechnology,* **16**, 2149.

[8] Kozlov G.I. 2003 *Tech.Phys.Let*., **29** (9), 787.

[9] Kurti J., ZolyomiV., Gruneis A., Kuzmany H. 2002 *Phys.Rev.B,* **65**, 165433.

[10] Bulgakova N.M., Bulgakov A.V., Svensson J., Campbell E.E.B. 2006, *Appl. Phys. A*, **85**, 109-116.